THE JOURNAL OF PHYSICAL CHEMISTRY B

Article

pubs.acs.org/JPCB

Impact of DNA Environment on the Intrastrand Cross-Link Lesions: Hydrogen Atom Release as the Last Step of Formation of G[8-5m]T

José Pedro Cerón-Carrasco,*[,†,‡] Denis Jacquemin,[‡,¶] and Elise Dumont*[,§]

[†]Departamento de Química Física, Universidad de Murcia, 30100 Murcia, Spain

[‡]CEISAM, UMR CNRS 6230, BP 92208, Université de Nantes, 2 Rue de la Houssinière, 44322 Nantes, Cedex 3, France

[¶]Institut Universitaire de France, 103 bd St Michel, 75005 Paris, Cedex 5, France

[§]Laboratoire de Chimie, UMR 5182 CNRS, École Normale Supérieure de Lyon, 46 allée d'Italie, 69364 Lyon, Cedex 07, France

ABSTRACT: Oxidative intrastrand cross-links where two nucleobases are covalently tethered form a particularly harmful class of DNA lesions. Their formation follows a radical pathway, as initiated by reactive oxygen species, which often ends with the departure of the hydrogen H8 of guanine to restore a closed-shell adduct. The ease of this abstraction step is investigated here for three systems of increasing complexity, C8-methyleguanine, the guanine-thymine dinucleoside monophosphate (GpT), and GpT embedded in a hexameric DNA sequence. First-principle calculations, combined with semiempirical approaches for the latter system, are performed to determine the energetics of the intermediates and to compare their respective exergonicities, which turned out to significantly depend on the environment. The hydrogen departure path is shown to be strongly favored compared to usual H-abstraction sites for normal guanine, while the impact of the biological environment is evidenced as the H8 departure becomes more difficult when larger structures are considered. A computational assessment of a plausible oxime intermediate is discussed as well.

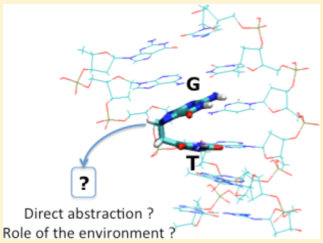

INTRODUCTION

DNA damage spans a large range of defects, whose formation pathways and structural signatures within B-DNA are not always easily studied. At this stage, the two probably most understood lesions are 8-oxo guanine[1] and cyclobutane pyrimidine dimers.[2,3] Indeed, a wealth of experimental data are available, whereas complementary modeling studies allowed one to provide a refined overall view of the underlying structures and reactivities related to these two lesions. It is now accepted that oxidative DNA lesions are usually formed upon multistep chemical reactions[4] that can be written down as a succession of elementary acts,[5] such as electron uptake,[6] hydroxyl attack,[7,8] hydrogen or proton transfer, and so forth.[9]

DNA defects mostly occur in its ground electronic state, though photoinduced pathways have also been evidenced.[10] The latter processes take place due to the DNA photosensitization by small organic or organometallic molecules that are able to induce a phototriggered electron transfer.[11,12] For radical pathways, most computational studies rely on density functional theory (DFT) approaches, which has been proven to provide valuable insights into the complex and competitive chemistry of DNA damages.[8,13−15] These simulations are usually performed on isolated fragments, with an implicit solvation model or microhydrated environment.[4,16] It has also recently become possible to treat explicitly solvated model systems, resorting to combined quantum mechanics/molecular mechanics (QM/MM) descriptions eventually coupled to molecular dynamics (MD). For instance, the process of hydroxyl radical abstraction of a hydrogen atom on guanine has been analyzed with such a hybrid theoretical scheme.[17] However, QM/MM approaches or combined quantum mechanics/semiempirical methods (so-called QM/SE formalism) also afford a more realistic description of DNA because short oligonucleotides can be handled. We underline that the B-helical environment has been proven to decisively affect the features of tandem DNA lesions, where two nucleobases become covalently tethered.[18] Recently, the experimental focus has shifted from simple damages to much more complex lesions that are more rare but that concomitantly suffer from a lower repair rate.[19] The most-frequenly formed of such tandem lesions is the formation of a covalent bridge between a thymine and a guanine that takes place through a three-step mechanism schematized in Figure 1. The formation is initiated by (i) hydrogen abstraction on the solvent-exposed methyl group of thymine[20] followed by (ii) the attack from the so-formed radical T[$-CH_2$]$^\bullet$ onto the C8 atom of guanine, whereas (iii) the departure of the hydrogen atom H8 yields a close-shell DNA defect. We highlight that this third step is not, in a sense, a hydrogen departure because a reagent has to proceed to allow this abstraction. A complete view of the formation process of the oxidative intrastrand cross-links (ICLs) certainly constitutes an ambitious goal in the DNA damage research line, desirable because only a kinetic picture will provide a rationale for the experimental formation yields that have been reported so far, that is, 0.050 lesions per 10^9 nucleotides.[21]

While the two first steps of the above-described tandem lesion have been explored and are rather well-understood,[18,20] information on the H-abstraction remains scarce. The B-helical

Received: September 6, 2013
Revised: December 6, 2013
Published: December 6, 2013

dx.doi.org/10.1021/jp408947u | J. Phys. Chem. B 2013, 117, 16397−16404

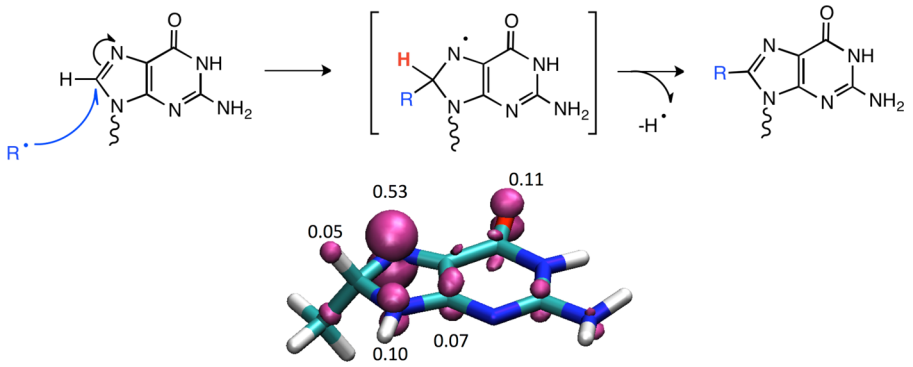

Figure 1. Mechanism for the radical attack onto guanine by a generic moiety R• and subsequent hydrogen departure (H8 displayed in red), this second step being studied herein. The wavy line denotes the *N*-glycosidic bond. The transient radical GHMe]• structure is known to be stable, with a radical character dominant on the nitrogen N7, as shown on the spin density plot.

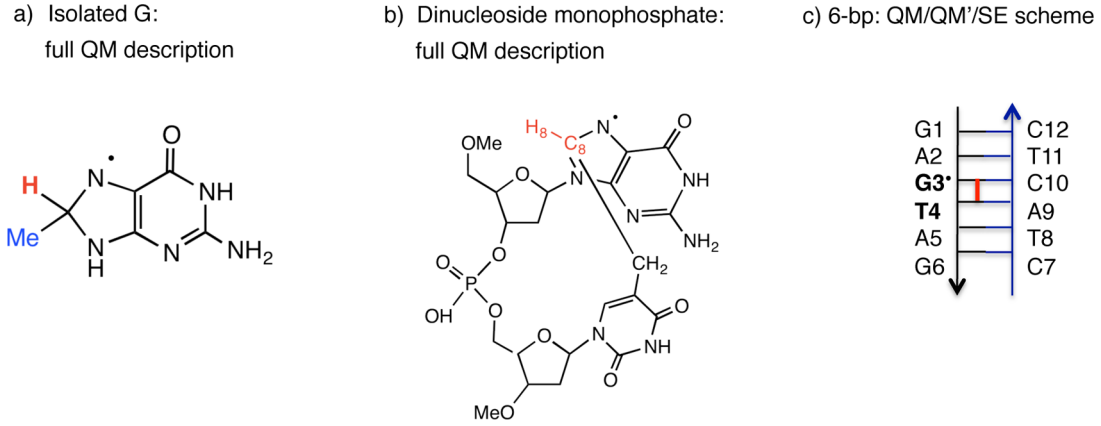

Figure 2. Three systems of increasing complexity considered in this study, (a) isolated guanine, (b) dinucleoside monophosphate (DM), and (c) GpT embedded in a 6-bp sequence.

macromolecular environment may be expected to play a role on the second step, the formation of the covalent bridge itself. This cyclization was studied recently by one of us, relying on hybrid QM/MM MD scheme,[22] and in that initial study, it was postulated that the first and third steps should be less affected by the presence of a macromolecular environment. In the present contribution, we challenge this assumption by estimating the energy profiles for the H8 departure using the three systems of increasing complexity represented in Figure 2. Guanine is the weak point in DNA oxidation as the formation of its radical cation is relatively easy. It has been proven that a B-DNA environment tunes its stability,[23] and it can be similarly expected that the (free) energy profile of H8-abstraction can be significantly tuned by the molecular environment. We report here a detailed investigation of the relative stabilities of both radical and neutral guanine-thymine stacked adducts, G[8-5m]T]• and G[8-5m]T, respectively, when the size of the molecular DNA environment is increased. The H-abstraction elementary act is also the last step in the formation of other lesions, for example, the formation of peroxyl adducts,[24] and, in a broader context, is of key importance for understanding the H-abstraction of antioxidant derivatives.[25,26] From a more methodological point of view, we note that, unlike steps (i) and (ii),[17,22] the final step can hardly be studied by relying on a QM/MM MD strategy. Indeed, due to the radical character of the species combined with a delocalization in the π-ring, the solvation of the molecules involved in step (iii) cannot be investigated with a classical force field. It requires a complete electronic description, and we make use here of our recently proposed sophisticated three-layers QM/QM′/SE scheme that allows treatment of such a chemical act with most realism.[27] Whereas computational studies of hydrogen abstraction are timely,[28] the surroundings are, for this reason, often discarded. Evidences of the importance of the DNA environment are scarce,[29] and the main scope of the contribution is clearly to shed light on this overlooked aspect.

METHODOLOGY

As illustrated in Figure 2, we have used several chemical models with increasingly detailed accounts of the biological environment, (a) a single methylated guanine base, (b) a stacked guanine-thymine dinucleoside monophosphate (DM), and (c) a rather complete six base pairs (6-bp) DNA sequence. The latter model is based on the equilibrated MD dodecamer duplex following a three-layered ONIOM[30] partition scheme as implemented in Gaussian09.[31] More specifically, the starting geometry was extracted from a subpart of a dodecamer featuring G[8-5m]T]• in its center, obtained by a QM/MM MD trajectory, which guarantees a relevant conformation of the G[8-5m]T]• within this hexameric sequence.[18] This structure is subsequently split into three regions or layers (high, medium, and low) that allow us to combine different theoretical approaches in the same calculation. The region of interest, namely, the two base pairs directly involved in the H-abstraction (high layer), and the two stacked base pairs (medium layer) are fully optimized at M06-2X/6-311G(d,p)

dx.doi.org/10.1021/jp408947u | J. Phys. Chem. B 2013, 117, 16397−16404

and M06-2X/6-31G(d) levels,[32,33] respectively. This functional has been shown to accurately describe the noncovalent interactions in biological problems.[34−37] The model is completed with the border base pairs and the lateral sugar−phosphate backbone (low layer) to mimic the real DNA environment. All atoms located in the low layer are frozen in space and treated with the less demanding PM6 semiempirical method.[38] The proposed partial optimization procedure retains the characteristic double helix form while allowing it to be flexible enough for exploring the DNA mutagenic mechanisms.[39,40] To further validate the predicted stabilities, the total energies have been recomputed with more extended atomic basis sets (including include diffuse functions). These single-point calculations include the effects of the aqueous media through the well-known polarizable continuum model (PCM)[41] so that the used level of theory can be shortened as PCM-(M06-2X/6-311++G(d,p):M06-2X/6-31+G(d):PM6)//M06-2X/6-311G(d,p):M06-2X/6-31G(d):PM6.

According to our MD and ONIOM simulations, no water molecules are in close contact with H8. Indeed, the first water molecule in the solvation sphere is located at ∼3 Å, while the second sphere includes four extra molecules at ∼5 Å, in clear contrast with the first hydration shell around the heteroatoms of the base pair that lie under the 2 Å threshold.[42−44] This finding suggests that the studied mutation process can be effectively described with an implicit solvent model as PCM because (i) the hydrophobic zone around the H8 reaction is large enough and (ii) it does not involve ionic intermediates. Nevertheless, the validity of this choice was confirmed by additional test calculations performed on microhydrated methyleguanine, DM, and the hexamer (see Table 1), demonstrating that the choice of the solvation model has a very limited impact on the estimated bond dissociation energy (BDE). Indeed, the differences reported in Table 1 are trifling compared to the modifications introduced when varying the size of the system.

Table 1. Bond Dissociation Free Energies for the C8···H8 Linkage (in kcal·mol^{-1}) As a Function of the Solvation Scheme[a]

	ΔE	ΔG
Isolated GHMe]$^{\bullet}$		
gas	31.4	19.6
PCM + 0 water	31.3	19.9
PCM + 1 water	31.3	19.3
PCM + 2 water	31.3	17.0
PCM + 3 water	31.9	19.2
DM GpT]$^{\bullet}$		
gas	13.2	10.2
PCM + 0 water	13.2	10.2
PCM + 1 water	13.5	10.6
PCM + 2 water	12.9	10.1
PCM + 3 water	13.7	11.2
6-bp System		
gas	35.5	31.3
PCM	40.4	36.2
PCM + diffuse functions	40.1	36.0
PCM + diffuse functions + 1 water	39.9	35.0

[a]Gas, implicit continuum description or microhydration.

RESULTS AND DISCUSSION

Intrinsic Ease of H-Abstraction in Guanine: Direct versus N7 Pathways. Let us first analyze the abstraction of the hydrogen atom H8 of the GHMe]$^{\bullet}$ radical to restore a closed-shell methylated guanine; this corresponds to the second step of Figure 1. This system is hereafter taken as model for a carbon-centered radical attack on G and hence for the subsequent formation of a covalent bridge through a radical pathway. The BDE for C8−H8 attains ΔE = 31.3 kcal·mol^{-1} (ΔG = 19.9 kcal·mol^{-1}) when evaluated by the following reaction

$$G{-}H{-}Me^{\bullet} \rightarrow G{-}Me + H^{\bullet}$$

This value clearly singles out with BDEs previously reported, at a similar level of theory, other possible sites of hydrogen abstraction.[8] Indeed, for closed-shell guanine, the hydrogen atoms most prone to departure are either on N2 or on N1 (i.e., on the exocyclic amino group and on the −NH− function), with BDEs close to 100 kcal·mol^{-1}. They were recomputed on GHMe]$^{\bullet}$ to allow comparisons on a perfectly equal footing. The data collated in Table 2 confirm that H8 indeed becomes the most favorable site of abstraction to restore a closed-shell methylated guanine. Indeed, abstraction of a hydrogen on N2 or N1 respectively corresponds to energies of 65.7 and 70.7 kcal·mol^{-1}.[45] This shows beyond reasonable doubt that hydrogen abstraction will occur preferably on the C8 position for the G[-Me]H]$^{\bullet}$. This electronic preference could nevertheless be modulated by both the characteristic interactions in the double DNA helix structure (e.g., π-staking) and the accessibility of the solvent in the vicinity of the C8 position.[20]

Table 2. Bond Dissociation Free Energies for the C8···H8 Linkage (in kcal·mol^{-1}) Evaluated on the Three Systems of Increasing Complexity[a]

site of H-abstraction	ΔE	ΔG
Isolated Guanine		
C8	123.1	107.8
N1	103.0	87.4
N2	102.6	86.6
Isolated GHMe]$^{\bullet}$		
C8	31.3	19.9
N1	65.7	50.4
N2	70.7	54.1
G[8-5m]T]$^{\bullet}$		
C8	13.2	10.2
6-bp System		
C8	40.4	36.2

[a]See representations in Figures 4 and 6. For isolated guanine and GHMe]$^{\bullet}$, we also report the BDEs for abstraction on N1 or on N2.

The spin density delocalization can be used to quantify the stability of a radical; a high concentration of the unpaired electron on one atom is consistent with an unstable (reactive) radical and vice versa. As shown in Figure 1, the spin density is delocalized mostly on the N7 atom (0.53 e) with only a minor contribution of the oxygen atom (0.11 e). This suggests a rather stable G[-Me]H]$^{\bullet}$ entity, as confirmed by the large energy associated with the C8···H8 dissociation process (ΔE=31.3 kcal·mol^{-1}). Indeed, a comparison with the first two other steps for the formation of G[8-5m]T points out that the cyclization is the most facile chemical act (ΔE = 16.2 kcal·mol^{-1}[35] and ΔG = 19.9 kcal·mol^{-1}), whereas the initiating H-

dx.doi.org/10.1021/jp408947u | J. Phys. Chem. B 2013, 117, 16397−16404

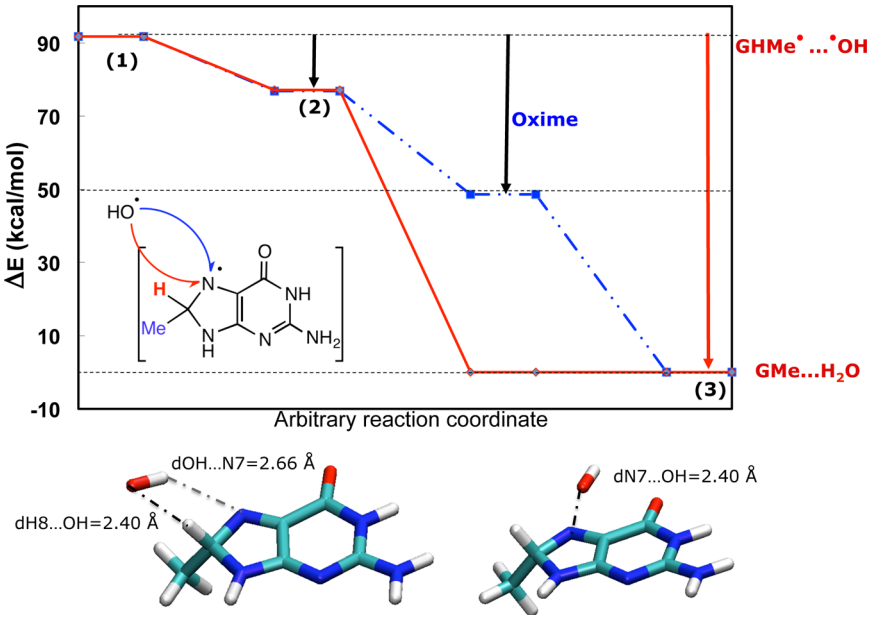

Figure 3. Energy profile for the hydrogen atom abstraction of [GHMe]• mimicked by adding a hydroxyl radical. The reference of energy is defined by the system composed of infinitely separated guanine and one proximal water molecule the stabilization due to the hydrogen bond accounting for 6 kcal·mol^{-1}. The two nearly isoenergetic structures (**2**) correspond to the approach of HO• at a distance of 2.4 Å. The red curve corresponds to the approach of HO• toward H8. The oxime intermediate lies 48.6 kcal·mol^{-1} above the GMe···H_2O product.

abstraction is more demanding energetically (ΔE = 96.8 kcal·mol^{-1} and ΔG = 81.6 kcal·mol^{-1}) and dominates the formation of the ICL, as proposed by Chatgilialoglu on (normal) guanine.[46] The spin densities plotted in Figure 1 also suggest the possibility of a free radical addition, for example, a hydroxyl on N7 to form an oxime. This species is characterized by a ═N(−OH)− motif, which is a known intermediate that undergoes dehydration to generate methylguanine alongside with one water molecule, according to the Beckmann rearrangement. Such addition may be favored based on an orbital picture, the overlap between the two lone pairs giving rise a σ-bonding orbital. The relative stability of this oxime can be properly quantified as we introduce a hydroxyl radical. As previously discussed by Sevilla and co-workers, the position of the hydroxyl is essential to rationalize the ease of an electron uptake.[8] Indeed, these authors demonstrated that the process is direct and barrierless.[8] Here, we adapt our model to describe not only the H8-abstraction but also the addition of the hydroxyl radical to the N7 atom. Specifically, one can also gain consistent insight on the most favored hydroxyl attack, N7 or H8, by constraining the two approaching distances. We have chosen an OH−GHMe]• distance of 2.4 Å here so that, on the one hand, no multiconfigurational character comes into play and, on the other hand, the triplet states can be discarded because they lie higher in energy. The energy profile given in Figure 3 illustrates the close competition between the two approaches, direct versus N7-indirect. Therefore, the possibility of forming an oxime undergoing a subsequent dehydration cannot be ruled out in the case of the isolated GHMe]• system. Indeed, the two structures (**2**) obtained by approaching HO• toward either H8 or N7 at a distance of 2.4 Å are nearly isoenergetic. We note that a weak interaction between the hydrogen atom of the hydroxyl and the N7 atoms takes place at a distance of 2.6 Å, which favors a syn orientation of this center. In line with Sevilla's analysis, it can be proposed that the position of the attacking radical determines the product that is formed, such that the hydrogen-abstraction process may not be direct but might partially proceed through an oxime intermediate.

The oxime lies energetically in the middle between the reactant GHMe]•···•OH and the product of dehydration, that is, the monohydrated C8-methyleguanine GMe···H_2O (respectively 91.7, 48.6, and 0.0 kcal·mol^{-1}), as can be seen in Figure 3. This marked decrease of energy favoring the dehydration is directly related to the subsequent gain of aromaticity. The relative stabilities of the structures (**1**), (**2**), and (**3**) and of the oxime can be expected to be significantly changed in B-DNA or even for the DM in the same way that the stability of the guanine radical cation is modulated by the DNA structure.[23] Experimental data are often inferred on DM reactivity and transferred to B-DNA situations,[47] but up to now, little is known concerning the validity of this "mapping", a point assessed in the next section.

GpT: Influence of π-Stacking and of the Deoxyribose−Phosphodiester−Deoxyribose Moiety. We now consider the impact of a thymine in the 5′ position on the ease of H8 atom abstraction of the guanine; this process corresponds to case (b) in Figure 2. The impact of the thymine arises both from the π-stacking and from the mechanical constraint due to the deoxyribose−phosphodiester−deoxyribose moiety. The DM environment does not affect the spin distribution of the initial G[8-5m]T]• radical; the radical is localized on the π-ring of the guanine, remaining like the one of the isolated GHMe]• in Figure 1 with a dominant contribution from N7 (0.55). This is consistent with the very limited fluctuations observed during the ab initio MD trajectory.[18] Despite these outcomes, the C8···H8 BDE is significantly decreased to ΔE = 13.2 kcal·mol^{-1} (ΔG = 10.2 kcal·mol^{-1}), such that the formation of the closed-shell d(G[8-5m]T) defect is thermodynamically facilitated, with a barrier roughly halved compared to the isolated case. This marked fall does not originate in additional electronic contributions but

dx.doi.org/10.1021/jp408947u | J. Phys. Chem. B 2013, 117, 16397−16404

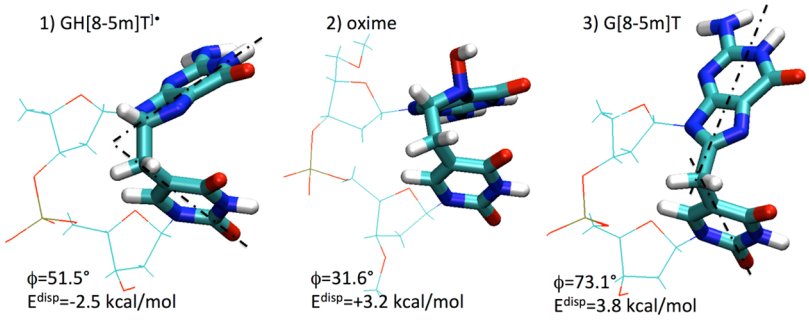

Figure 4. Cartoon representations for the three optimized structures characterizing the hydrogen abstraction on the G[8-5m]T• DM. The loss or gain in dispersion energy, E^{disp}, is computed with respect to the system featuring perfectly planar radical thymine T• and guanine as well as ideal angles for B-helicity.

rather reflects the large opening and deplanarization of the two nucleobases that the guanine-thymine ICL undergoes upon H8-abstraction (see Figure 4). The final structure can indeed be qualified as T-shaped, with a plane-to-plane ϕ angle, the angle between the normal vectors of the two nucleobases, of 73°. The driving force for this unfolding is the change of hybridization of the C8 atom that also implies a (partial) release of the mechanical strain of the deoxyoxyribose−phosphodiester−deoxyribose moiety. This contribution brings more stabilization than the loss of dispersion, evaluated to 3.8 kcal·mol^{-1}. The marked conformational flexibility of DMs has been recently emphasized in a (classical) MD study,[48] with free energy barriers between open and π-stacked structures lower than 1 kcal·mol^{-1}. In short, the facilitated H8-abstraction ($\Delta\Delta E$ of −18.1 kcal·mol^{-1} in the DM system) compared to the isolated model does not arise from a difference of spin delocalization, which remains intrinsic, but from the mechanical embedding, clearly exemplifying that the hydrogen removal is not insensitive to the medium. In fact, it is the abstraction of the hydrogen that induces the change of the hybridization of the C8 atom and, in turn, drives the unfolding.

In contrast, the oxime adduct remains much higher in energy than the final monohydrated ICL, with an increment of ΔE = 66.8 kcal·mol^{-1}, which is significantly higher than the value obtained on the isolated system (ΔE = 48.6 kcal·mol^{-1}). We underline that the oxime intermediate can adopt a more planar conformation, with an angle ϕ of ∼30°. In line with this geometrical feature, the gain in the dispersion energy compared to the reactant is 5.7 kcal·mol^{-1}. The enantiomer of the oxime presenting the hydroxyl group pointing toward the O4 oxygen atom of the thymine was also considered and found to be 3.0 kcal·mol^{-1} above the structure depicted in Figure 4 ($\Delta\Delta G$ = 3.5 kcal·mol^{-1}); a hydrogen bond can be formed but implies a loss a π-stacking, so that the total effect remains rather small. A second argument in favor of the direct hydrogen abstraction is the anisotropy of the hydroxyl approach as the thymine is placed in the 3′ position. The two structures optimized while imposing an approaching distance of 2.4 Å either toward H8 or N7 are given in Figure 5. At this distance, the approach toward H8 is favored by 6.5 kcal·mol^{-1} as the hydroxyl is "guided" by additional weak interactions between HO• and one of the hydrogen atoms of the methylene bridge, whereas the hydrogen of the hydroxyl develops another stabilizing interaction with the oxygen atom of the capping group in 5′. These two interactions give rise to effective hydrogen bonds as HO• gets closer to H8. Meanwhile, the approach toward N7 does not benefit from any specific stabilization.[49] Consequently, the oxime pathway appears to be significantly disfavored in the DM environment.

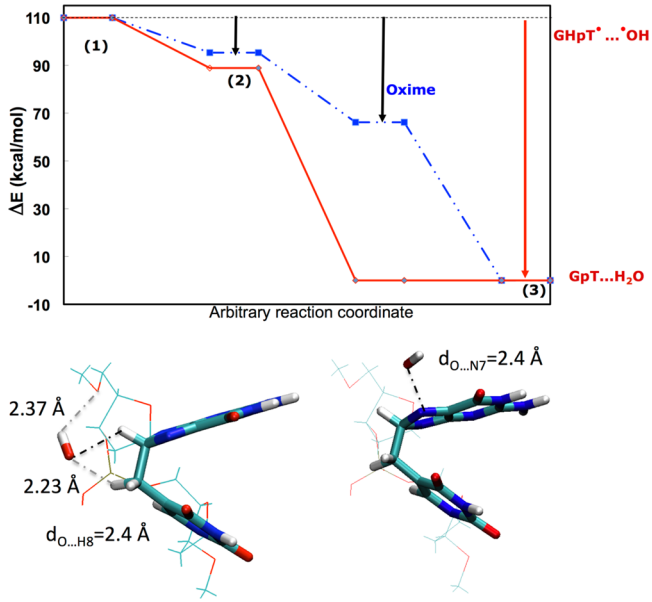

Figure 5. Energy profile for the hydrogen atom abstraction of H8 on the G[8-5m]T]• DM. The direct abstraction pathway (in red) is favored. The oxime lies 66.8 kcal·mol above the final monohydrated ICL.

At this stage, we have strong evidence that the hydrogen abstraction is significantly environment-dependent. Several extra possible effects may obviously come into play: the π-stacking that can be almost completely annihilated and the distortion undergone by the full system that can be very large. With these two first models (isolated and DM), it is not clear how the abstraction reaction takes place in B-DNA. Indeed, in a realistic environment, one expects the Watson−Crick pairing and the surrounding nucleobases to favor more planar structure than in DM while imposing many more constraints than in the free GHMe. Consequently, in the next paragraph, we inspect the structures of the G[8-5m]T• and G[8-5m]T within a double-stranded duplex.

Stabilities within a 6-bp System. We investigate here the hydrogen abstraction taking place in our model of B-DNA. The BDE is 40.4 kcal·mol^{-1}, 9.1 kcal·mol^{-1} higher compared to that of the isolated guanine and therefore much larger than that in the DM model. This increase mostly reflects a distortion of the B-DNA environment. The optimized structures of the G[8-5m]T• and G[8-5m]T defects embedded in the 6-bp sequence are depicted in Figure 6A. A first striking feature is that the plane-to-plane angle ϕ no longer comes close to orthogonality

dx.doi.org/10.1021/jp408947u | J. Phys. Chem. B 2013, 117, 16397−16404

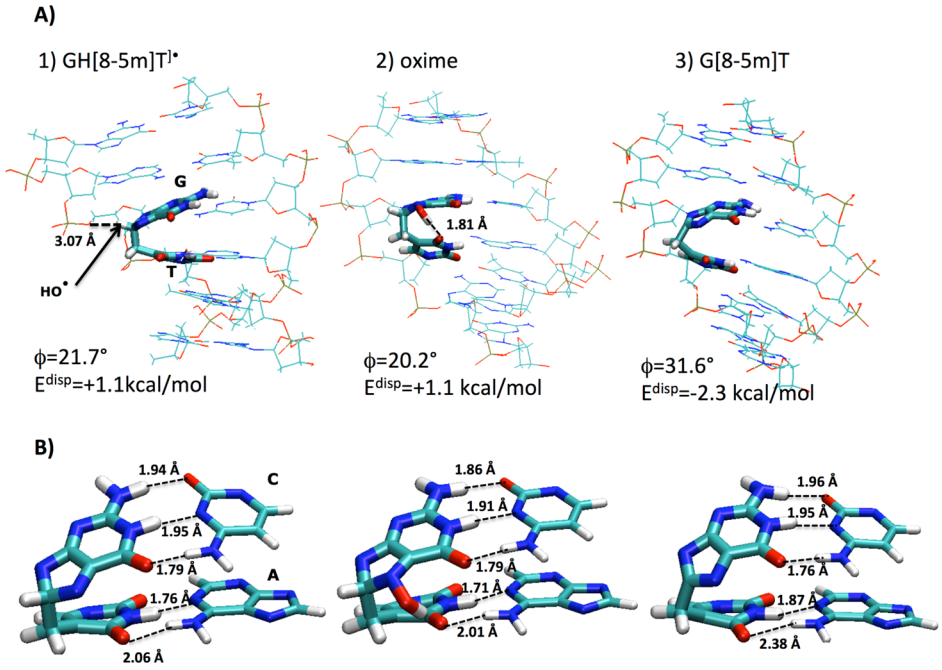

Figure 6. (A) Optimized geometries for the G[8-5m]T•, the oxime intermediate, and the G[8-5m]T embedded in a 6-bp ds sequence. (B) View of the Watson−Crick pairing between G[8-5m]T and the opposite nucleobases is given.

in the final closed-shell defect due to the mechanical embedding of the B-helix that impedes a more pronounced opening (values of ϕ reach 21.7 and 31.6° of the radical and the H8-abstract moieties, respectively). The plane-to-plane opening would be penalized due to the disruption of both π-stacking and Watson−Crick pairing; the π-stacking is globally maintained, with an energetic penalty for the London forces only that does not overpass 2.3 kcal·mol^{-1}.

We underline that the values of ϕ for the embedded GH[8-5m]T]• and G[8-5m]T almost perfectly match the data obtained in our previous QM/MM MD study[18] and confirm the relevance of the static B-DNA model used here. The guanine can accommodate a rather marked "pinch" with a constraint on C8 while maintaining a qualitatively near-identical but quantitatively slightly weakened Watson−Crick pairing with the cytosine, as illustrated in Figure 6B. The thymine experiences a larger tilt, which induces an almost complete disruption of the hydrogen bond between the O2 oxygen atom of thymine and the amino group located at A9 on the opposite strand.

Our computational scheme, which includes eight nucleobases at a quantum level, also indicates with no ambiguity that there is no delocalization of the spin density onto A2, in sharp contrast to the well-studied charge-transfer stabilization of the guanine radical cation G$^{+\bullet}$.[23] In Figure 7, the relative stabilities of the guanine-centered, H8-containing radical and the oxime are compared. In B-DNA, the oxime is found to be 18.1 kcal·mol^{-1} higher in energy, and this constitutes a marked difference. We note that the oxime points toward the thymine, forming a hydrogen bond with the O2 oxygen atom with this base (distance of 1.81 Å). Yet, most of the stabilization comes from the conformational constraints exerted on the final product.[50] The stability of the oxime is such that one cannot isolate an optimized structure for the approach of HO• toward H8 at a distance of 2.4 Å. This result suggests that the oxime pathway may significantly come into play in the real-life case. This is corroborated by the fact that the entry of a hydroxyl free

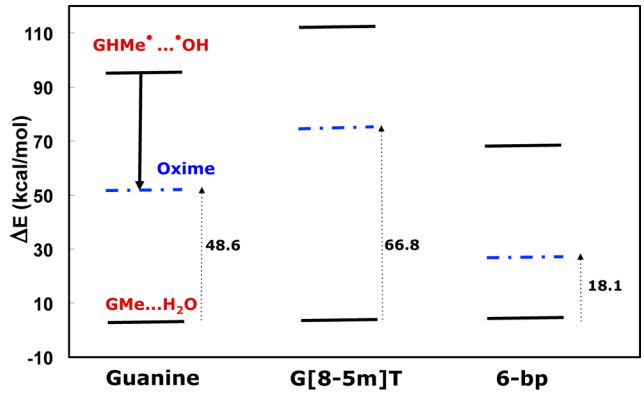

Figure 7. Relative stabilities of the guanine radical GHR•, the oxime (dashed line), and the final GR[-H] adduct.

radical or a water molecule in the vicinity of H8 is strongly penalized/blocked by the phosphate group linking G and A2. In Figure 6A, the distance between H8 and the vicinal oxygen atom of the phosphate group attains 3.07 Å, whereas the $-CH_2-$ moiety is much more exposed to the solvent.

CONCLUDING REMARKS

In this work, we investigated with state-of-the-art computational approaches the hydrogen atom abstraction on the radical intermediate G[8-5m]T]• as the last but nontrivial step behind the formation of tandem DNA lesions. Our theoretical predictions confirm that the H8 departure is not an energetically easy chemical act and are fully consistent with the recent data reordered in the pulse radiolysis experiments by Chatgilialoglu and co-workers, who proposed the H-atom-abstraction processes as the dominating mechanism in the reaction of the hydroxyl radical with the guanine bases. Moreover, our simulations allow us to go further in showing that the last step of the formation process of intrastrand cross-links shall not be discarded. Paradoxically, the H8-abstraction

dx.doi.org/10.1021/jp408947u | J. Phys. Chem. B 2013, 117, 16397−16404

turns out to be more dependent on the environment than the G ← T• cyclization, for which a simplified model can be chosen to study the formation of oxidative intrastrand lesions.[15] The marked sensitivity to its medium of this hydrogen abstraction arises from the subsequent dehybridization of the C8 atom, notably inducing an important B-helix structural distortion. Using a simplified model can be misleading for elementary acts surrounding the radical attack. Here, we show that the final reaction in the multistep pathway is less solvent-accessible than the initial steps, which can be expected to increase the lifetime of the transient G[8-5m]T•. To go further, one would need to resort to an adaptative QM/MM MD view to statistically derive ratios for the different approaches. Indeed, the position of the hydroxyl is determinant, and our data suggest a possible competition between the direct H-abstraction and the passage through an oxime intermediate. A dynamic framework would also allow characterization of the (first-shell) solvation in the vicinity of the covalent linkage formed between guanine and thymine, and we intend to pursue that direction.

AUTHOR INFORMATION

Corresponding Authors

*E-mail: jpceron@um.es (J.P.C.-C.).
*E-mail: elise.dumont@ens-lyon.fr (E.D.)

Notes

The authors declare no competing financial interest.

ACKNOWLEDGMENTS

This work was partly performed within the framework of the LABEX PRIMES (ANR-11-LABX-0063) of Université de Lyon, within the program "Investissements d'Avenir" (ANR-11-IDEX-0007) operated by the French National Research Agency (ANR). J.P.C.-C. acknowledges the support from the FP7 EU Marie Curie Actions through the Campus Mare Nostrum 37/38 CMN UMU Incoming Mobility Programme ACTion (U-IMPACT). D.J. acknowledges the European Research Council (ERC) and the *Région des Pays de la Loire* for financial support in the framework of a Starting Grant (Marches - 278845) and a *recrutement sur poste stratégique*, respectively. Calculations were performed using the local HPC resources of PSMN at ENS-Lyon, on GENCI-CINES/IDRIS, on the CCIPL (*Centre de Calcul Intensif des Pays de Loire*), and of CEISAM's Troy cluster.

REFERENCES

(1) Fortini, P.; Pascucci, B.; Parlanti, E.; D'Errico, M.; Simonelli, V.; Dogliotti, E. 8-Oxoguanine DNA Damage: At the Crossroad of Alternative Repair Pathways. *Mutat. Res.* **2003**, *531*, 127−139.
(2) Sinha, R. P.; Hader, D.-P. UV-Induced DNA Damage and Repair: A Review. *Photochem. Photobiol. Sci.* **2002**, *1*, 225−236.
(3) Cadet, J.; Berger, M.; Douki, T.; Morin, B.; Raoul, S.; Ravanat, J.; Spinelli, S. Effects of UV and Visible Radiation on DNA — Final Base Damage. *Biol. Chem.* **1997**, *378*, 1275−1286.
(4) Sviatenko, L.; Gorb, L.; Hovorun, D.; Leszczynski, J. Interaction of 2-Deoxyadenosine with *cis*-2-Butene14dial: Computational Approach to Analysis of Multistep Chemical Reactions. *J. Phys. Chem. A* **2012**, *116*, 2333−2342.
(5) Duncan Lyngdoh, R. H.; Schaefer, H. F. Elementary Lesions in DNA Subunits: Electron, Hydrogen Atom, Proton, and Hydride Transfers. *Acc. Chem. Res.* **2009**, *42*, 563−572.
(6) Loos, P.-F.; Dumont, E.; Laurent, A. D.; Assfeld, X. Important Effects of Neighbouring Nucleotides on Electron Induced {DNA} Single-Strand Breaks. *Chem. Phys. Lett.* **2009**, *475*, 120−123.
(7) Cadet, J.; Delatour, T.; Douki, T.; Gasparutto, D.; Pouget, J.-P.; Ravanat, J.-L.; Sauvaigo, S. Hydroxyl Radicals and {DNA} Base Damage. *Mutat. Res., Fundam. Mol. Mech. Mutagen.* **1999**, *424*, 9−21.
(8) Kumar, A.; Pottiboyina, V.; Sevilla, M. D. Hydroxyl Radical (OH) Reaction with Guanine in an Aqueous Environment: A DFT Study. *J. Phys. Chem. B* **2011**, *115*, 15129−15137.
(9) Florian, J.; Leszczynski, J. Spontaneous DNA Mutations Induced by Proton Transfer in the Guanine.Cytosine Base Pairs: An Energetic Perspective. *J. Am. Chem. Soc.* **1996**, *118*, 3010−3017.
(10) Atherton, S. J.; Harriman, A. Photochemistry of Intercalated Methylene Blue: Photoinduced Hydrogen Atom Abstraction from Guanine and Adenine. *J. Am. Chem. Soc.* **1993**, *115*, 1816−1822.
(11) Cuquerella, M. C.; Lhiaubet-Vallet, V.; Cadet, J.; Miranda, M. A. Benzophenone Photosensitized DNA Damage. *Acc. Chem. Res.* **2012**, *45*, 1558−1570.
(12) Chantzis, A.; Very, T.; Daniel, C.; Monari, A.; Assfeld, X. Theoretical Evidence of Photo-Induced Charge Transfer from {DNA} to Intercalated Ruthenium (II) Organometallic Complexes. *Chem. Phys. Lett.* **2013**, *578*, 133−137.
(13) Zhang, R. B.; Eriksson, L. A. Effects of OH Radical Addition on Proton Transfer in the Guanine-Cytosine Base Pair. *J. Phys. Chem. B* **2007**, *111*, 6571−6576.
(14) Labet, V.; Morell, C.; Grand, A.; Cadet, J.; Cimino, P.; Barone, V. Formation of Cross-Linked Adducts between Guanine and Thymine Mediated by Hydroxyl Radical and One-Electron Oxidation: A Theoretical Study. *Org. Biomol. Chem.* **2008**, *6*, 3300−3305.
(15) Dupont, C.; Patel, C.; Ravanat, J. L.; Dumont, E. Addressing the Competitive Formation of Tandem DNA Lesions by a Nucleobase Peroxyl Radical: a DFT-D Screening. *Org. Biomol. Chem.* **2013**, *11*, 3038−3045.
(16) Cerón-Carrasco, J. P.; Jacquemin, D.; Cauët, E. Cisplatin Cytotoxicity: A Theoretical Study of Induced Mutations. *Phys. Chem. Chem. Phys.* **2012**, *14*, 12457−12464.
(17) Abolfath, R. M.; Biswas, P. K.; Rajnarayanam, R.; Brabec, T.; Kodym, R.; Papiez, L. Multiscale QM/MM Molecular Dynamics Study on the First Steps of Guanine Damage by Free Hydroxyl Radicals in Solution. *J. Phys. Chem. A* **2012**, *116*, 3940−3945.
(18) Garrec, J.; Patel, C.; Rothlisberger, U.; Dumont, E. Dumont, E. Insights into Intrastrand Cross- Link Lesions of DNA from QM/MM Molecular Dynamics Simulations. *J. Am. Chem. Soc.* **2012**, *134*, 2111−2119.
(19) Bergeron, F.; Auvré, F.; Radicella, J. P.; Ravanat, J.-L. HO* Radicals Induce an Unexpected High Proportion of Tandem Base Lesions Refractory to Repair by DNA Glycosylases. *Proc. Natl. Acad. Sci. U.S.A.* **2010**, *107*, 5528−5533.
(20) Balasubramanian, B.; Pogozelski, W. K.; Tullius, T. D. *Proc. Natl. Acad. Sci. U.S.A.* **1998**, *95*, 9738−9743.
(21) Hong, H.; Cao, H.; Wang, Y. Formation and Genotoxicity of a Guanine−Cytosine Intrastrand Cross-Link Lesion In Vivo. *Nucleic Acids Res.* **2007**, *35*, 7118−7127.
(22) Patel, C.; Garrec, J.; Dupont, C.; Dumont, E. What Singles Out the G[8-5]C Intrastrand DNA Cross-Link? Mechanistic and Structural Insights from Quantum Mechanics/Molecular Mechanics Simulations. *Biochemistry* **2013**, *52*, 425−431.
(23) Gervasio, F. L.; Laio, A.; Iannuzzi, M.; Parrinello, M. Influence of DNA Structure on the Reactivity of the Guanine Radical Cation. *Chem.—Eur. J.* **2004**, *10*, 4846−4852.
(24) Hong, I. S.; Carter, K. N.; Sato, K.; Greenberg, M. M. Characterization and Mechanism of Formation of Tandem Lesions in DNA by a Nucleobase Peroxyl Radical. *J. Am. Chem. Soc.* **2007**, *129*, 4089−4098.
(25) Luzhkov, V. B. Mechanisms of Antioxidant Activity: The DFT Study of Hydrogen Abstraction from Phenol and Toluene by the Hydroperoxyl Radical. *Chem. Phys.* **2005**, *314*, 211−217.
(26) Yoshida, T.; Hirozumi, K.; Harada, M.; Hitaoka, S.; Chuman, H. *J. Org. Chem.* **2011**, *76*, 4564−4570.
(27) Cerón-Carrasco, J. P.; Jacquemin, D. Interplay between Hydroxyl Radical Attack and H-Bond Stability in Guanine-Cytosine. *RSC Adv.* **2012**, *2*, 11867−11875.

(28) Mujika, J. I.; Uranga, J.; Matxain, J. M. Computational Study on the Attack of $^{\bullet}$OH Radicals on Aromatic Amino Acids. *Chem.—Eur. J.* **2013**, *19*, 6862−6873.
(29) Qi, C.; Liu, F.; Eriksson, L.; Zhang, R. Insight into Reaction Mechanism and Product Formation a C8-Purine Radical in RNA: A Theoretical Perspective. *Theor. Chem. Acc.* **2013**, *132*, 1−10.
(30) Dapprich, S.; Komáromi, I.; Byun, K. S.; Morokuma, K.; Frisch, M. J. A New ONIOM Implementation in Gaussian 98. Part 1. The Calculation of Energies, Gradients and Vibrational Frequencies and Electric Field Derivatives. *J. Mol. Struct.: THEOCHEM* **1999**, *462*, 1−21.
(31) Frisch, M. J.; et al. *Gaussian 09*, revision A.02; Gaussian Inc.: Wallingford, CT, 2009.
(32) Zhao, Y.; Truhlar, D. G. Density Functionals with Broad Applicability in Chemistry. *Acc. Chem. Res.* **2008**, *41*, 157−167.
(33) Zhao, Y.; Truhlar, D. G. The M06 Suite of Density Functionals for Main Group Thermochemistry, Thermochemical Kinetics, Noncovalent Interactions, Excited states, and Transition Elements: Two New Functionals and Systematic Testing of Four M06-Class Functionals and 12 Other Functional. *Theor. Chem. Acc.* **2008**, *120*, 215−241.
(34) Hohenstein, E. G.; Chill, S. T.; Sherrill, C. D. Assessment of the Performance of the M05-2X and M06-2X Exchange−Correlation Functionals for Noncovalent Interactions in Biomolecules. *J. Chem. Theory Comput.* **2008**, *4*, 1996−2000.
(35) Dupont, C.; Patel, C.; Dumont, E. Improved DFT Description of Intrastrand Cross-Link Formation by Inclusion of London Dispersion Corrections. *J. Phys. Chem. B* **2011**, *115*, 15138−15144.
(36) Cerón-Carrasco, J. P.; Jacquemin, D. Electric Field Induced DNA Damage: An Open Door for Selective Mutations. *Chem. Commun.* **2013**, *49*, 7578−7580.
(37) Churchill, C. D. M.; Wetmore, S. D. Developing a Computational Model That Accurately Reproduces the Structural Features of a Dinucleoside Monophosphate Unit within B-DNA. *Phys. Chem. Chem. Phys.* **2011**, *13*, 16373−16383.
(38) Stewart, J. J. P. Optimization of Parameters for Semiempirical Methods V: Modification of NDDO Approximations and Application to 70 Elements. *J. Mol. Model.* **2007**, *13*, 1173−1213.
(39) Chen, H.-Y.; Kao, C.-L.; Hsu, S. C. N. Proton Transfer in Guanine-Cytosine Radical Anion Embedded in B-Form DNA. *J. Am. Chem. Soc.* **2009**, *131*, 15930−15938.
(40) Cerón-Carrasco, J. P.; Zúñiga, J.; Requena, A.; Perpète, E. A.; Michaux, C.; Jacquemin, D. Combined Effect of Stacking and Solvation on the Spontanoues Mutation in DNA. *Phys. Chem. Chem. Phys.* **2011**, *13*, 14584−14589.
(41) Tomasi, J.; Mennucci, B.; Cammi, R. Quantum Mechanical Continuum Solvation Models. *Chem. Rev.* **2005**, *105*, 2999−3094.
(42) Schneider, B.; Berman, H. M. Hydration of the DNA Bases Is Local. *Biophys. J.* **1995**, *69*, 2661−2669.
(43) Auffinger, P.; Westhof, E. Water and Ion Binding around RNA and DNA (C,G) Oligomers. *J. Mol. Biol.* **2000**, *300*, 1113−1131.
(44) Makarov, V.; Pettitt, B.; Feig, M. Solvation and Hydration of Proteins and Nucleic Acids: A Theoretical View of Simulation and Experiment. *Acc. Chem. Res.* **2002**, *35*, 376−384.
(45) It was verified that triplet states lie higher in energy.
(46) Chatgilialoglu, C.; D′Angelantonio, M.; Guerra, M.; Kaloudis, P.; Mulazzani, Q. G. A Reevaluation of the Ambident Reactivity of the Guanine Moiety Towards Hydroxyl Radicals. *Angew. Chem., Int. Ed.* **2009**, *48*, 2214−2217.
(47) Budzinski, E. E.; Maccubbin, A. E.; Evans, M. S.; Kulesz-Martin, M.; Box, H. C. Analysis of DNA Damage at the Dinucleoside Monophosphate Level: Application to the Formamido Lesion. *Radiat. Res.* **1992**, *132*, 288−295.
(48) Jafilan, S.; Klein, L.; Hyun, C.; Florian, J. Intramolecular Base Stacking of Dinucleoside Monophosphate Anions in Aqueous Solution. *J. Phys. Chem. B* **2012**, *116*, 3613−3618.
(49) On the cartoon representation, the hydrogen of the hydroxyl can rotate with a barrier of 3 kcal·mol^{-1} due to a repulsion with H8.
(50) The conformation where the oxime points up, towards the adenine A2, is found to be higher in energy.